Surface Science 700 (2020) 121681

Contents lists available at ScienceDirect

Surface Science

journal homepage: www.elsevier.com/locate/susc

Nonlocal friction forces in the particle-plate and plate-plate configurations: Nonretarded approximation

G.V. Dedkov*, A.A. Kyasov

Nanoscale Physics Group, Kabardino-Balkarian State University, Nalchik, Russia

ARTICLE INFO

Keywords:
Van der Waals friction
quantum friction
Casimir-lifshitz forces
nonlocal effects

ABSTRACT

In the nonrelativistic approximation of fluctuation electrodynamics, using the specular reflection model and the nonlocal dielectric permittivity of a metal, we obtained simple analytical expressions for the friction forces in the particle-plate and plate-plate systems upon relative motion of the bodies with constant velocity. It is shown that at separations of about $1 \div 10$ *nm*, for an Au nanoparticle (or a gold plate) moving near another gold plate at rest, the dissipative forces are 2 to 4 orders of magnitude higher than in the case when the local Drude dielectric permittivity is used.

1. Introduction

A rigorous description of the fluctuation-electromagnetic (FEM) friction and dissipative effects in nanostructures is of great fundamental and practical importance in connection with the intensive development of micro- and nanotechnology, since these effects may affect the behaviour of micromechanical devices (MEMS) [1]. However, until recently, theoretical calculations of these effects caused a lot of discussion even for the simplest configurations of particle — plate and plate — plate (see Refs. 2–4 and the corresponding references). In contrast to the measurements of the static conservative van der Waals and Casimir-Lifshitz forces [5,6], experimental measurements of the relevant dissipative (friction) forces are still at the initial stage. In the latter case, as shown in Refs. 6,7, the role of the spatial dispersion (SD) effect is relatively small, but in the case of quantum friction, spatial dispersion has a much stronger influence on the friction force magnitude [8,9]. This is due, in particular, to the possibility of generating electron-hole pairs when interacting bodies are in relative motion even at a low speed.

The aim of this work is to calculate the van der Waals friction force (FEM friction at a nonzero temperature T) and quantum friction force (FEM friction at $T = 0$) with a more detailed justification of the approach based on using the specular reflection model (SRM) [10,11,12,17] and the nonrelativistic approximation ($c \to \infty$) of fluctuation electrodynamics in the case of arbitrary temperatures and direction of motion of a small particle relative to a thick plate. In particular, SRM is known to reproduce many properties of real surfaces and it was successfully used when calculating the energy losses of energetic ions near a solid surface and the dynamics of electrons captured by the wake potential [13].

Based on these results, the case of the interaction of two plates in relative motion is treated using the "correspondence principle" between the particle–plate and plate–plate configurations [14]. Unlike [8,9], where the authors explored the quantum friction between two plates and an atom with a surface at $T = 0$, the use of a realistic analytical approximation for the nonlocal dielectric function of a metal enables performing analytical and numerical calculations of the quantum friction force and van der Waals friction force at an arbitrary temperature T in a much simpler way.

2. Theoretical formulation

Coordinate system used and a schematic representation of the specular reflection model corresponding to a particle with fluctuating dipole moment $\mathbf{d}(t)$ moving relative to the surface of a polarizable metal plate are shown in Fig. 1. In vacuum region $z > 0$, the electric field is created by the dipole $\mathbf{d}(t)$ with Cartesian components $(V_x,0, -V_z)$ of the velocity vector $\mathbf{V}$, its mirror image $\mathbf{d}'(t)$, mirror-symmetric relative to the plane $z = 0$ (with components $(V_x,0, V_z)$ of the velocity vector $\mathbf{V}'$ and other components), and a fictitious charge density $\rho_s(x,y,t)\delta(z)$ on the plane $z = 0$ fixed by the boundary conditions. In the case of moving charged particles, the SRM construction was described in detail in Refs. 11, 12.

The field inside the plate ($z < 0$) is also created by the charge density $\rho_s(x,y,t)\delta(z)$. By setting the polarization vectors of the dipole sources in the form $\mathbf{P} = \mathbf{d}(t)\delta(\mathbf{r} - \mathbf{V}t)$ and $\mathbf{P}' = \mathbf{d}'(t)\delta(\mathbf{r} - \mathbf{V}'t)$ (with $\mathbf{d} = (d_x, d_y, d_z)$ and $\mathbf{d}' = (d_x, d_y, -d_z)$), decomposing the electric

* Corresponding author.
E-mail address: gv_dedkov@mail.ru (G.V. Dedkov).

https://doi.org/10.1016/j.susc.2020.121681
Received 31 January 2020; Received in revised form 14 June 2020; Accepted 19 June 2020
Available online 20 June 2020
0039-6028/

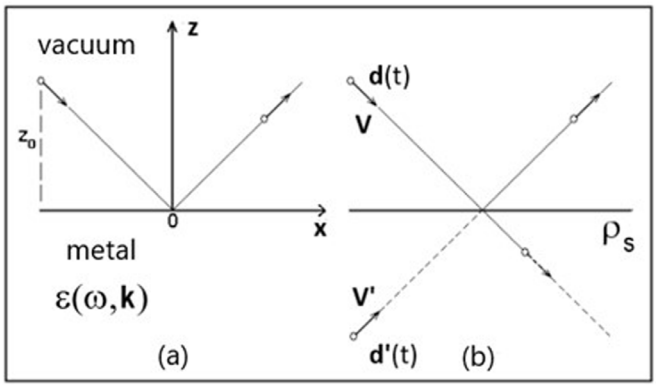

Fig. 1. (a) A particle with fluctuating dipole moment **d**(t), being reflected at $t = 0$ from the surface and the Cartesian coordinate system used. (b) Schematic representation of the fluctuating dipoles and charges used in the specular reflection model to calculate the induced potential in vacuum.

potential and the corresponding charge densities $-\,\mathrm{div}\mathbf{P}$, $-\,\mathrm{div}\mathbf{P}'$, $\rho_s(x,y,t)\delta(z)$ into Fourier integrals with respect to frequency ω and three-dimensional wave vector $\mathbf{k} = (\mathbf{q}, k_z) = (k_x,k_y,k_z)$, solution of the Poisson equations $\Delta\Phi = -4\pi\rho$ for the Fourier components of the potential at $z > 0$ and $z < 0$ can be written as

$$\Phi(\omega, k) = -\frac{4\pi}{k^2}[\mathrm{i}\mathbf{kd}(\omega - \mathbf{kV}) + \mathrm{i}\mathbf{kd}(\omega - \mathbf{kV}) + \rho_s(\omega, q)], z > 0. \quad (1)$$

$$\Phi(\omega, \mathbf{k}) = \frac{4\pi\rho_s(\omega, q)}{k^2\varepsilon(\omega, \mathbf{k})}, z < 0. \quad (2)$$

where $\mathbf{d}(\omega - \mathbf{kV})$, $\mathbf{d}(\omega - \mathbf{kV}')$ and $\rho_s(\omega,q)$ are the Fourier-components of the dipole moments and $\rho_s(x,y,t)$. The continuity condition for potential Φ at the boundary $z = 0$ determines the quantity $\rho_s(\omega,q)$:

$$\rho_s(\omega, q) = -\frac{q}{\pi + ql_0}\int_{-\infty}^{\infty}\frac{dk_z}{q^2+k_z^2}[\mathrm{i}\mathbf{kd}(\omega - q_xV_x + k_zV_z) + \mathrm{i}\mathbf{kd}(\omega - q_xV_x - k_zV_z)]$$
$$= -\frac{\pi}{\pi + ql_0}[\mathrm{i}\mathbf{qd}(\omega_+ - q_xV_x) + \mathrm{i}\mathbf{qd}(\omega_- - q_xV_x) + qd_z(\omega_+ - q_xV_x) + qd_z(\omega_- - q_xV_x)] \quad (3)$$

$$I_0 = \int_0^{\infty}\frac{dk_z}{k^2\varepsilon(\omega, \mathbf{k})'}, \quad (4)$$

where $\omega_{\pm} = \omega \pm \mathrm{i}qV_z$. When calculating integral (3), it is considered as the limit at $z \to 0$ from the same expression with additional factor $\exp(\mathrm{i}k_zz)$ in the integrand, and the integration over k_z is performed along a contour including the real axis and the upper semicircle of the complex plane. It should be noted that the proposed option of SRM in the case of fluctuating dipoles differs from that in Ref. 15, where the form $\mathbf{kd} = \mathbf{qd} - ik_zd_z$ was used in order to regularize the term in (3) involving the component d_z of an image dipole moment. If such a recipe is used, we obtain the twice lower numerical factor for the FEM friction force in the reference case of local dielectric permittivity.

The boundary condition for the continuity of induction at the boundary $z = 0$ is satisfied automatically, since the component of potential (1) with a Fourier term due to the contribution of dipoles is symmetric with respect to the boundary $z = 0$ and has a zero derivative with respect to the z coordinate, and the contributions of fictitious charges to induction are dropped out at $z \to \pm 0$. In the framework of SRM, any charge distribution associated with a moving particle has the same property. The Fourier component $\Phi^{ind}(\omega,\mathbf{k})$ of the potential induced in the vacuum region is found from $\Phi(\omega, \mathbf{k})$ by subtracting the Fourier component $\Phi^{vac}(\omega,\mathbf{k})$ of the potential for a particle moving in vacuum. In order to do this, we should make the replacement $\varepsilon(\omega, \mathbf{k}) \to 1$ in (1) –(4) . As a result, we obtain

$$\Phi^{ind}(\omega, \mathbf{k}) = \frac{2\pi}{k^2}\Delta(\omega, q)\cdot[\mathrm{i}\mathbf{qd}(\omega_+ - q_xV_x) + \mathrm{i}\mathbf{qd}(\omega_- - q_xV_x) + qd_z(\omega_+ - q_xV_x) + qd_z(\omega_- - q_xV_x)], \quad (5)$$

$$\Delta(\omega, q) = \frac{\pi - qI_0}{\pi + qI_0}. \quad (6)$$

Taking into account (5), the expression for the induced potential at the point $(\mathbf{r}, t) = (\mathbf{R}, z, t) = (x, y, z, t)$ in the vacuum region takes the form

$$\Phi^{ind}(\mathbf{R}, z, t) = \frac{1}{(2\pi)^4}\int d\omega d^2q dk_z\Phi^{ind}(\omega, \mathbf{k})\exp(i(\mathbf{qR} + k_zz - \omega t)). \quad (7)$$

When a particle moves parallel to the surface, substituting (5) into (7), one needs to use the limit $V_z \to 0$, $V_x \to V$ under the condition $V_zt \to \pm z_0$, where z_0 is the particle distance from the surface. After that, integrating (7) by k_z in the same way as in (3), we obtain the Fourier component of the potential with a decomposition by frequency and a two-dimensional wave vector

$$\Phi^{ind}(\omega, q, z) = \frac{2\pi}{q}\Delta(\omega, q)e^{-q(z+z_0)}\left[\mathrm{i}q_xd_x(\omega - q_xV) + iq_yd_y(\omega - q_xV) + qd_z(\omega - q_xV)\right]. \quad (8)$$

Formula (8) fully coincides with the exact solution of the electrodynamic problem in the case of parallel motion, when local dielectric permittivity ε(ω) is used [15].

Using (8), further calculation of the dissipative van der Waals force follows the way of the calculation with local ε(ω). The starting equation for the force acting on a particle is given by

$$\mathbf{F} = (\langle\mathbf{d}^{sp}\mathbf{E}^{ind}\rangle + \langle\mathbf{d}^{ind}\mathbf{E}^{sp}\rangle) \quad (9)$$

where $\mathbf{d}^{sp,ind}$ and $\mathbf{E}^{sp,ind}$ are the spontaneous and induced components of the dipole moment and the electric field, the angular brackets denote the quantum-statistical averaging. The projections of **F** on the x, z axes correspond to the friction force and the force of attraction to the surface (dynamic van der Waals force). The first correlator in the right-hand side of (9) is calculated via the standard fluctuation-dissipation relation for the components of the dipole moment $\mathbf{d}^{sp}$. In the second correlator, the induced dipole moment $\mathbf{d}^{ind}$ is expressed through $\mathbf{E}^{sp}$and the atomic polarizability, and the fluctuation-dissipation relation for the field components is used (see Refs. 3, 15).

Expressing the dielectric response of the particle via the frequency-dependent polarizability α(ω), we obtain the following result for F_x with T_1 and T_2 being the local particle and plate temperatures in the units of energy, $\omega_+ = \omega + q_xV$)

$$F_x = -\frac{\hbar}{\pi^2}\int_0^{\infty}d\omega\int_{-\infty}^{+\infty}dq_xq_x\int_{-\infty}^{+\infty}dq_yqe^{-2qz_0}\mathrm{Im}\Delta(\omega, q)\mathrm{Im}\alpha(\omega_+)[\coth(\hbar\omega/2T_2) - \coth(\hbar\omega_+/2T_1)] \quad (10)$$

It is worthwhile noting that the concept of local or total thermal equilibrium in a dynamical nonequilibrium situation is not trivial (see Ref. 16, for example), but currently, the construction with two local temperatures is actively used. [3,4,21]

In the linear approximation in velocity and $T_1 = T_2 = T$, from (10) it follows

$$F_x = -\frac{1}{2\pi}\left(\frac{\hbar^2V}{T}\right)\int_0^{\infty}d\omega\int_0^{\infty}dqq^4e^{-2qz_0}\mathrm{Im}\Delta(\omega, q)\mathrm{Im}\alpha(\omega)\sinh^{-2}(\hbar\omega/2T) \quad (11)$$

and in the limit of quantum friction ($T = 0$), respectively,

$$F_x = \frac{4\hbar}{\pi^2}\int_0^\infty dq_x q_x \int_0^\infty dq_y q e^{-2qz_0}\int_0^{q_x V} d\omega \mathrm{Im}\alpha(\omega - q_x V)\mathrm{Im}\Delta(\omega, q). \quad (12)$$

Formulas (10) – (12), quite naturally, completely coincide with the known results in the case of the local dielectric permittivity of plate materials [2-4].

3. Spherical particle above metal surface

For the practical calculation of the force F_x by formulas (11), (12), we use the expression for the polarizability $\alpha(\omega) = R^3(\varepsilon(\omega) - 1)/(\varepsilon(\omega) + 2)$ of a spherical particle with radius R and the Drude dielectric constant $\varepsilon(\omega) = 1 - \omega_p^2/\omega(\omega + i\gamma)$, where ω_p and γ are the plasma frequency and the damping factor ($\omega_p = 9\ eV$ and $\gamma = 30\ meV$ for gold). For the function $\varepsilon(\omega, \mathbf{k})$ of the metal plate, we use the well-known approximation [18], which takes into account the linear-frequency asymptotic behaviour of the Lindhard permittivity, the generation of electron-hole pairs and plasmons (this is in line with the hydrodynamic approximation)

$$\varepsilon(\omega, \mathbf{k}) = 1 - \frac{\omega_p^2}{\{s^2k^2[1 - i\pi\omega\theta(2k_F - k)/2kV_F] - \omega(\omega + i\gamma)\}} \quad (13)$$

where k_F is the Fermi wave vector, $s = V_F/3$, V_F is the Fermi velocity, $\theta(x)$ is the unit Heaviside function. In this case, the low-frequency expansion of the integral (4) leads to the expression $I_0 = A + B + C$, where

$$A = \pi k_{TF}^{-1}(1 + x^2)^{-3/2}, \quad (14)$$

$$B = -i\left(\frac{\pi}{k_{TF}}\right)\left(\frac{\omega}{\omega_p}\right)\left[\frac{(2 + x^2)}{2(1 + x^2)^{3/2}}\ln\left(\frac{p\sqrt{1 + x^2} + \sqrt{p^2 - x^2}}{p\sqrt{1 + x^2} - \sqrt{p^2 - x^2}}\right) - \frac{p\sqrt{p^2 - x^2}}{(1 + p^2)\sqrt{1 + x^2}}\right]\theta(p - x), \quad (15)$$

$$C = -i\left(\frac{\pi}{k_{TF}}\right)\left(\frac{\gamma\omega}{\omega_p^2}\right)\left[\frac{\sqrt{1 + x^2} - x}{x\sqrt{1 + x^2} + x} - \frac{1}{2(1 + x^2)^{3/2}}\right]. \quad (16)$$

Here $x = q/k_{TF}$, $k_{TF} = \sqrt{3}\omega_p/V_F$ is the inverse Thomas-Fermi screening length, $p = 2k_F/k_{TF} = \sqrt[3]{3\pi^2/2}\sqrt{a_B/r_s}$, a_B and r_s are the Bohr radius and the jellium parameter ($r_s/a_B = 3.01$ and $p = 1.415$ for gold). We also mean one and the same value γ in $\varepsilon(\omega)$ and in (13). It should be noted that Eq. (15) is somewhat different from that presented in Ref. 11 (the expression in square brackets and the presence of $\theta(p - x)$). However, the difference is not crucial for the results. With allowance for (6) and (14)–(16) we obtain

$$\Delta(\omega, q) = \frac{1 - (\omega/\omega_p)^2S^2(x) + 2i(\omega/\omega_p)S(x)\sqrt{1 + x^2}}{(\sqrt{1 + x^2} + x)^2 + (\omega/\omega_p)^2S^2(x)}, \quad (17)$$

$$S(x) = \left[\frac{x(2 + x^2)}{2(1 + x^2)}\ln\left(\frac{p\sqrt{1 + x^2} + \sqrt{p^2 - x^2}}{p\sqrt{1 + x^2} - \sqrt{p^2 - x^2}}\right) - \frac{xp\sqrt{p^2 - x^2}}{(1 + p^2)\sqrt{1 + x^2}}\right]\theta(p - x) + \beta\left[\sqrt{1 + x^2} - x - \frac{2}{2(1 + x^2)}\right]. \quad (18)$$

In (18), and hereinafter, we omitted the small argument $\beta = \gamma/\omega_p$ in writing $S(x)$ for simplicity. In the case of low particle velocities $V \ll V_F$ and $S(x) \sim 1$ (V_F is the Fermi velocity), the terms proportional to ω^2 in (17) can be ignored, since only low frequencies $\omega \ll \omega_p$ contributes to integrals (11), (12). Similarly, for Imα one can use a simpler expression $\mathrm{Im}\alpha \approx 3i\gamma\omega/\omega_p^2$. Then, as a result of integration over frequency ω, formulas (11), (12) are reduced to

$$F_{x,T}^{(nl)}(z_0) = -\frac{\pi}{8}\left(\frac{R}{z_0}\right)^3\frac{\hbar\gamma}{z_0^2}\left(\frac{T}{\hbar\omega_p}\right)^2\frac{V}{\omega_p}f_1(2k_{TF}z_0) \quad (19)$$

$$F_{x,q}^{(nl)}(z_0) = -\frac{1}{256\pi}\left(\frac{R}{z_0}\right)^3\frac{\hbar\gamma}{z_0}\left(\frac{V}{\omega_p z_0}\right)^3 f_2(2k_{TF}z_0) \quad (20)$$

$$f_1(x) = \int_0^\infty dz\ z^4e^{-z}S_1(z/x), \quad (21)$$

The function $f_2(x)$ is given by (21) when replacing $z^4 \to z^6$.

$$S_1(x) = S(x)\frac{\sqrt{1 + x^2}}{(\sqrt{1 + x^2} + x)^2}. \quad (22)$$

If the local Drude function is used in calculating F_x, then $\Delta(\omega, q) \to (\varepsilon(\omega) - 1)/(\varepsilon(\omega) + 1)$ and performing elementary integration in (11), (12) yields

$$F_{x,T}^{(l)}(z_0) = -3\pi\left(\frac{R}{z_0}\right)^3\frac{\hbar\gamma}{z_0^2}\left(\frac{T}{\hbar\omega_p}\right)^2\frac{V}{\omega_p}\frac{\gamma}{\omega_p} \quad (23)$$

$$F_{x,q}^{(l)}(z_0) = -\frac{45}{16\pi}\left(\frac{R}{z_0}\right)^3\left(\frac{T}{\omega_p z_0}\right)^3\frac{\hbar\gamma}{z_0}\frac{\gamma}{\omega_p} \quad (24)$$

Comparing the fractions $F_{x,T}^{(nl)}/F_{x,T}^{(l)}$ and $F_{x,q}^{(nl)}/F_{x,q}^{(l)}$ corresponding to (19), (23) and (20), (24), we see that the increase in the friction force due to SD is mainly due to the presence of the large parameter $1/\beta = \omega_p/\gamma \gg 1$. This is in agreement with Ref. 9.

Fig. 2 shows the calculated ratio $F_x^{(nl)}/F_x^{(l)}$ depending on $2k_{TF}z_0$ for the force of quantum friction (dashed line) and friction at a finite temperature (solid line). It is worth noting that in the case of gold we have $2k_{TF}z_0 = 34$ at $z_0 = 1\ nm$. As follows from Fig. 2, the effect of SD leads to an increase in the dissipative van der Waals force by more than two orders of magnitude at $z_0 = 1 \div 10\ nm$.

4. Two plates in relative motion

As Lifshitz first showed [16], there is a simple "rule-of-thumb" between plate-plate (1) and particle-plate (2) configurations. This enables

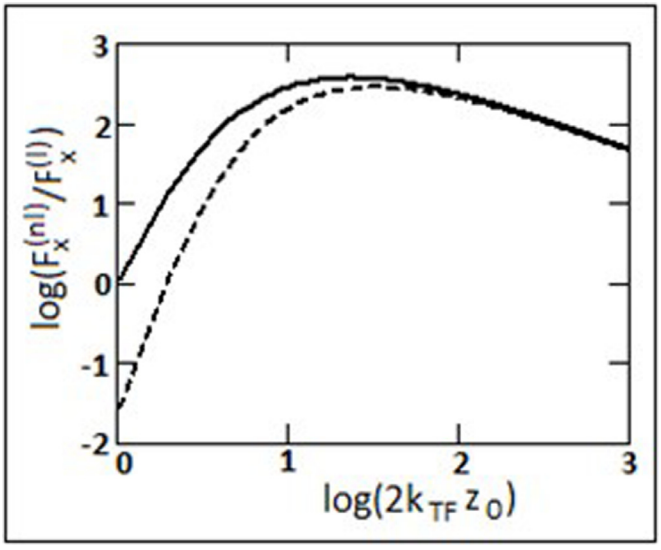

Fig. 2. Dependence $F_x^{(nl)}/F_x^{(l)}$ as a function of reduced distance $2k_{TF}z_0$ for an Au nanoparticle above the surface of gold. Dashed line: quantum friction force, solid line: friction force at a finite temperature; (nl) –nonlocal approximation (Eqs. (19), (20)), (l) –local approximation (Eqs. (23), (24)). The log functions hereinafter are with basis 10. For gold, $2k_{TF}z_0 = 34$ at $z_0 = 1\ nm$.

calculating the Casimir-Polder force in configuration 2 using the corresponding expression for the force in configuration 1. The rule reads

$$\Delta(\omega) \to 2\pi n\alpha(\omega) \tag{25}$$

$$F^{(2)}(z) = -\frac{1}{nS}\frac{d}{dl}F^{(1)}(l)_{l=z} \tag{26}$$

where α(ω) is the polarizability of a particle of a rarified medium with density n of particles that models the material of one of the plates, and S is the surface area of the plates in a vacuum contact.

In systems out of thermal and dynamic equilibrium, in the nonretarded limit, the corresponding transition rule was established in Refs. 3, 14. It was proved that relations (25), (26) are valid for all other quantities describing the FEM interaction, such as the rate of heat exchange and friction force. Such a correspondence rule, obviously, must be valid in the nonlocal case too, for a limiting transition from the nonlocal case to the local one to exist. In addition, relations (25), (26) can be applied for both transitions: from configuration 1 to configuration 2 and vice versa. At first sight, the validity of the opposite transition $F^{(2)} \to F^{(1)}$ with the presence of "reflection denominator" in the expression for $F_x^{(1)}(l)$ is not obvious. However, in addition to relations (25), (26), it is based on the transformation properties between the normal (lateral) projections of the forces $F_{x,z}^{(1,2)}$ and the rates of heating $dQ^{(1,2)}/dt$ within each configuration (in the nonretarded limit), and the fact that we have exact expressions for these quantities, known from solving one and the same electrodynamic problem in each configuration [3,14] .

With this in mind, to take SD in configuration 1 into account, one should use the replacement $\Delta(\omega) \to \Delta(\omega, q)$ in (9). It is worth noting that the above approach is different from that used in the calculations of the Casimir-Lifshitz attraction and friction forces with allowance for SD [4,6], where the authors used the nonlocal Lindhard- Mermin dielectric permittivity $\varepsilon(\omega, \mathbf{k})$ (Ref. 19) in the expressions for the amplitudes of reflection of electromagnetic waves. The difference is due to the fact that Eq. (6) for $\Delta(\omega, q)$ calculated in the framework of SRM can not be obtained by inserting $\varepsilon(\omega, \mathbf{k})$ into the reflection factor for P-waves.

In our case, the friction force acting on moving plate 1 per unit surface of the vacuum contact is formally the same as in Ref. 3 provided that $\Delta_1(\omega_+) \to \Delta_1(\omega_+, q)$ and $\omega_+ = \omega + q_x V$:

$$F_x(l) = -\frac{\hbar}{4\pi^3}\int_0^\infty d\omega \int_0^\infty d^2q q_x e^{-2ql}\mathrm{Im}\Delta_1(\omega_+, q)\mathrm{Im}\Delta_2(\omega, q)\,|D|^{-2}$$

$$\cdot\,[\coth(\hbar\omega/2T_2) - \coth(\hbar\omega_+/2T_1)] \tag{27}$$

where $D = 1 - \Delta_1(\omega_+, q)\Delta_2(\omega, q)\exp(-2ql)$ and l is the spacing between interacting plates. Using (27), the expressions for the friction force in a linear approximation in velocity (at $T_1 = T_2 = T$) and in the case of quantum friction ($T = 0$) take the form ($n(\omega) = 1/(\exp(\hbar\omega/T) - 1)$ is the Planck factor)

$$F_x(l) = \frac{\hbar V}{2\pi^3}\int_0^\infty d\omega\frac{dn(\omega)}{d\omega}\int_0^\infty d^2q q_x e^{-2ql}\mathrm{Im}\Delta_1(\omega, q)\mathrm{Im}\Delta_2(\omega, q)\,|D|^{-2} \tag{28}$$

$$F_x(l) = \frac{\hbar V}{2\pi^3}\int_0^\infty dq_y \int_0^\infty dq_x q_x e^{-2ql}\int_0^{q_x V} d\omega\mathrm{Im}\Delta_1(\omega - q_x V, q)\mathrm{Im}\Delta_2(\omega, q)\,|D|^{-2} \tag{29}$$

It is worth noting that in contrast to (27) and (29), the D-factor in (28) reads $D = 1 - \Delta_1(\omega, q)\Delta_2(\omega, q)\exp(-2ql)$. Formulas (28), (29) agree with those obtained by many authors [2-4,15,21] using local $\varepsilon(\omega)$, while (29) fully coincides with Eq. (24) in Ref. 8, obtained in the framework of the nonlocal quantum field theory.

As in Sec. 3, in the case under consideration ($V \ll V_F$), we can omit the terms proportional to ω^2 in Eq. (16). Then $\Delta_{1,2}(\omega, q) \cong 1$ and $\mathrm{Im}\Delta_{1,2}(\omega, q) \cong 2(\omega/\omega_p)S_1(x)$, and substituting these relations into (28), (29) yields (assuming that both plates are of the same material)

i) $T_1 = T_2 = T$

$$F_{x,T}^{(nl)}(l) = -\frac{1}{24}\left(\frac{T}{\hbar\omega_P}\right)^2\left(\frac{\hbar V}{l^4}\right)f_3(2k_{TF}l). \tag{30}$$

ii) $T_1 = T_2 = 0$

$$F_{x,q}^{(nl)}(l) = -\frac{1}{2^{11}\cdot 3}\left(\frac{V}{\omega_p l}\right)^3\left(\frac{\hbar\omega_p}{l^3}\right)f_4(2k_{TF}l). \tag{31}$$

$$f_3(x) = \int_0^\infty dy y^3 e^{-y}\frac{S_1^2(y/x)\left(\sqrt{1 + (y/x)^2} + (y/x)\right)^4}{\left[\left(\sqrt{1 + (y/x)^2} + (y/x)\right)^4 - e^{-y}\right]^2} \tag{32}$$

The function $f_4(x)$ is given by (32) when replacing $y^3 \to y^5$.

On the other hand using the local Drude function $\varepsilon(\omega) = 1 - \omega_p^2/\omega(\omega + i\gamma)$, we have $\Delta_{1,2}(\omega) \cong 1$, $\mathrm{Im}\Delta_{1,2}(\omega) \cong 2(\omega\gamma/\omega_p^2)$. Substituting these relations into (28), (29) yields

$$F_{x,T}^{(l)}(l) = -\frac{\zeta(3)}{4}\left(\frac{T}{\hbar\omega_p}\right)^2\left(\frac{\hbar V}{l^4}\right)\left(\frac{\gamma}{\omega_p}\right)^2, \tag{33}$$

$$F_{x,q}^{(l)}(l) = -\frac{5\zeta(5)}{2^8}\left(\frac{V}{\omega_p l}\right)^3\left(\frac{\hbar\omega_p}{l^3}\right)\left(\frac{\gamma}{\omega_p}\right)^2. \tag{34}$$

where $\zeta(3) = 1.202$ and $\zeta(5) = 1.037$ are the Riemann zeta-functions.

Shown in Fig. 3 are the calculated ratios $F_{x,T}^{(nl)}/F_{x,T}^{(l)}$ and $F_{x,q}^{(nl)}/F_{x,q}^{(l)}$ depending on $2k_{TF}l$, for two gold plates in relative motion. One can see that in the range $l = 1 \div 10$ nm, friction forces increase by four orders of magnitude if SD is accounted for. The effect is due to the large factor ω_p^2/γ^2.

5. Discussion

It is expedient to perform a more thorough comparison of the numerical values of forces F_x obtained using different approaches. Fig. 4 shows a linear in velocity friction force between two plates of gold, as a function of separation l for $T_1 = T_2 = 300\,K$, $V = 1m/s$.

Solid curve in Fig. 4 shows the nonlocal approximation, Eq. (30). The dashed-dotted curve (S-local Drude) and the curve shown by dots (P-local Drude) show the results with local Drude function, performed using a recently transformed formula of the Rytov-Levin-Polevoy theory

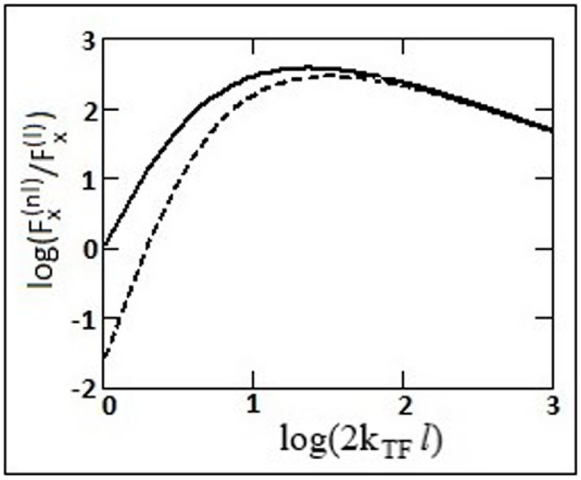

Fig. 3. Dependence $F_x^{(nl)}/F_x^{(l)}$ as a function of reduced distance $2k_{TF}l$ for two plates of gold in relative motion Dashed line: quantum friction force, solid line: friction force at a finite temperature; (nl) –nonlocal approximation Eqs. (30), ((31)), (l) –local approximation Eqs. (33), ((34)).

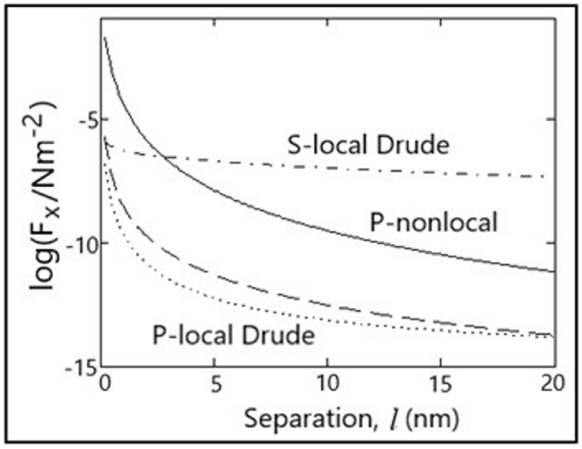

Fig. 4. Friction force between two gold plates at $T_1 = T_2 = 300\,K$, $V = 1 m/s$. Curve P-nonlocal: Eq. (30); curve S-local Drude: Eq. (A2), the second term (the contribution from S-waves); curve P-local Drude: Eq. (A2), the first term (the contribution from P-waves); dotted line: Eq. (33).

[21] (see Eq. (A2) in the Appendix and Ref. 22). These curves correspond to the contributions of the second and first terms in square brackets of (A2). It is worth noting that in (A2), both evanescent and propagating modes are accounted for, though at short separations l under consideration, the propagating modes make a small contribution to the result. The dashed curve shown in Fig. 4 was calculated by Eq. (33) and corresponds to the nonretarded local Drude approximation. We see that SD has a large effect only at short separations $l < 2\,nm$, whereas at larger l the local Drude approximation due to the modes with S- polarization is dominant. All the curves in Fig. 4 obeys the law $F_x \sim V$, but the $l -$ dependence is different: $F_x \sim l^{-5}$ for P-nonlocal Drude, $F_x \sim l^{-0.9}$ for S-local Drude, whereas for other two curves we have $F_x \sim l^{-4}$.

Fig. 5 compares the quantum friction forces at $T = 0$. The solid curve was calculated by Eq. (31). The dashed-dotted curve (local Drude) was calculated by Eq. (A3) with account of both P-waves and S-waves. Curve P-local Drude corresponds to the contribution from P-waves only (Eq. (A3), the first term). The values of the force calculated by Eq. (34) nearly coincide with those for P-local Drude curve, and these results are not shown. We see that the range of distances with strong SD effect ($l < 8\,nm$) is greater than in the case of "thermal friction" (Fig. 4). The solid curve (P-local Drude) obeys the law $F_x \sim V^3/l^{7.2}$ at $1 < l < 2\,nm$ and $F_x \sim V^3/l^2$ at $2 < l < 20\,nm$. The local Drude curve obeys the law $F_x \sim V^3/l^{3.2}$ at $1 < l < 2\,nm$ and $F_x \sim V^3/l^2$ at $2 < l < 20\,nm$.

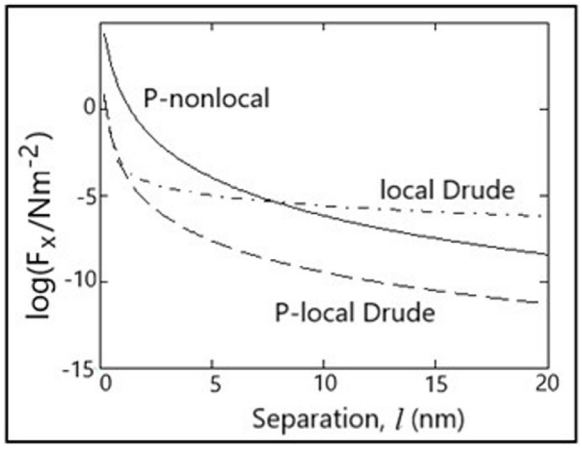

Fig. 5. Quantum friction force for two flat gold plates in parallel motion as a function of separation l at $V = 0.1V_F$ ($V_F = 1.4 \cdot 10^6\,m/s$) . Solid curve (P-nonlocal): Eq. (31), curve local Drude: Eq. (A3) (summary contribution from S-waves and P-waves), dashed curve (P-local Drude) corresponds to the contribution from P-waves in (A3). The curve calculated by Eq. (34) (nonretarded local Drude for P-waves) is very close to P-local Drude curve and is not shown.

We also compared the results with Ref. 8 (i.e. in the case of quantum friction, $F \sim V^3$), using two reference points in Fig. 8(a,b) of this paper corresponding to $V/V_F = 0.2$ and separation distances of 1.27 nm (24 a_0) and 5.3 nm (100 a_0). The jellium parameter ($r_s = 3\,a_B$) in Ref. 8 is close to our's ($r_s = 3.01\,a_B$). According to these data, $F_x \approx 9\,N/m^2$ and $F_x \approx 0.004\,N/m^2$, whereas Eq. (31) yields $F_x = 10.8\,N/m^2$ and $F_x \approx 0.0055\,N/m^2$, i.e. the matching is quite good.

Despite the "positive" influence of SD at small separations, the absolute values of the friction forces are still very small. For example, in an ideal sphere-plane configuration, $F_{sp} \approx \pi R a F_z(a,V)$, where R and a are the curvature radius of the probing tip and the minimum separation distance, even at $R = 100\,\mu m$, $V = 300\,m/s$ ($T = 300K, a = 1nm$) we find by Eq. (30) $F_{sp} = 3 \cdot 10^{-15} N$ at $F_z = 0.01\,N/m^2$. In turn, in typical experimental situation, when the AFM technique is used, even this rather "moderate" velocity value requires a very large product of oscillation amplitude A and frequency f ($2\pi Af = 300\,m/s$). The high values of A, R, along with the small separation distance, make such an experiment very difficult. Probing the quantum friction force is still more difficult, since at $V = 300\,m/s$ we obtain a much lower value $F_z = 6 \cdot 10^{-8}\,N/m^2$, or we should increase the velocity to about $10^5 m/s$. In Ref. [23], the author reported on resonance effects in the friction force and radiative heat emission at relative sliding of two polar dielectric plates (SiO_2, SiC) with velocities of 10^4–10^5 m/s. In our case of metal plates with local Drude and nonlocal (Eq. (13) dielectric permittivities, we did not find any resonances at these velocities, since the value V/a is much less than an important frequency of metals. The case $V/a \sim \omega_p$ requires special consideration.

Finally, it is worthwhile to discuss the role of temperature. According to Eq. (30), the nonlocal friction force scales as $F_x \sim T^2$ and decreases with decreasing temperature. Since the dissipation mechanism at SD is mostly due to the electron-hole excitation, this is quite natural. As for the general local theory [22], our recent numerical calculations showed an unexpectedly sharp growth in the friction force at $T < 50\,K$, when the damping factor γ in the Drude formula for $\varepsilon(\omega)$ obeys the Bloch-Grüneisen law, $\gamma \sim T^5$. Perhaps, this is due to some interference of the temperature–dependant quantities in the formula for F_x. This low-temperature behaviour is an intriguing issue and should be studied more thoroughly.

6. Conclusion

In this paper, we provide a derivation of the van der Waals friction force on a particle (thick metal plate) moving at constant velocity parallel to another thick metal plate (configurations 1 and 2). The theory is a generalization of the specular reflection model and the FEM theory with account of the spatial dispersion of the material of the plate. Using the analytical approximation for the bulk dielectric permittivity $\varepsilon(\omega, \mathbf{k})$ of a metal, we obtained closed analytical expressions for the friction forces at a finite temperature T and in the case of quantum friction ($T = 0$). When obtaining expressions for the friction force in the configuration of parallel plates, we used the principle of correspondence between configurations 1 and 2. This provides an unambiguous limit transition between formulas obtained in local and nonlocal theory.

Comparison of nonlocal and local formulations shows that the van der Waals friction force calculated using the nonlocal approach is 2–4 orders of magnitude higher than using the local approach (both for quantum friction and friction at a finite temperature). Mathematically, the increase in friction is due to the large factor ω_P/γ. This is in agreement with Refs. 8,9. Moreover, a comparison of the numerical values of the nonlocal quantum friction force with those obtained in Ref. 8 within the quantum-field theory formalism, shows a very good

coincidence.

The main theoretical result of this paper is that it provides a simple analytical approach for calculating the van der Waals friction force at separations between the bodies of order several nm, using a model expression for the dielectric permittivity of materials, which takes into account the frequency and spatial dispersion.

Author statement

We revised our MS according to the comments made by reviewers. The sites of correction in the text are shown in red. Figs. 1, 3,4 were redrawn. Several linguistic corrections have been done. We are thankful to both referee for very fruitful points of improvement. The points of correction are described below.

Declaration of Competing Interest

None.

Supplementary materials

Supplementary material associated with this article can be found, in the online version, at doi:10.1016/j.susc.2020.121681.

Appendix A

In Ref. 20, based on the original Rytov-Levin-Polevoy theory with local $\varepsilon(\omega)$[21], we obtained a general expression for the friction force in configuration of two parallel thick plates with account of retardation (the corresponding quantities relating to plates 1 and 2 have the subscripts 1,2) at $V/c \ll 1$

$$F_x = -\frac{\hbar}{4\pi^3}\int_0^\infty d\omega \int d^2k k_x |q|^2 [\mathrm{Im}(q_1/\varepsilon_1)\mathrm{Im}(\widetilde{q}_2/\widetilde{\varepsilon}_2)|Q_\varepsilon|^{-2} + \mathrm{Im}(q_1/\mu_1)\mathrm{Im}(\widetilde{q}_2/\widetilde{\mu}_2)|Q_\mu|^{-2}] \quad \text{(A1)}$$

$$[\coth(\hbar\omega_-/2T_2) - \coth(\hbar\omega/2T_1)]$$

where $q = \sqrt{k^2 - (\omega/c)^2}$, $q_1 = \sqrt{k^2 - \varepsilon_1\mu_1(\omega/c)^2}$, $q_2 = \sqrt{k^2 - \varepsilon_2\mu_2(\omega/c)^2}$, the tilde means that the corresponding arguments of $\varepsilon_{1,2}$ and $\mu_{1,2}$ (dielectric permittivities and magnetic permeabilities) are taken at $\omega_- = \omega - k_x V$. Eq. (A1) describes the friction force acting on plate 1 that moves in the $x-$ direction with constant velocity V. Moreover, in (A1) we have $Q_\varepsilon = (q + q_1/\varepsilon_1)(q + \widetilde{q}_2/\widetilde{\varepsilon}_2)\exp(ql) - (q - q_1/\varepsilon_1)(q - \widetilde{q}_2/\widetilde{\varepsilon}_2)\exp(-ql)$, and Q_μ is described by the same expression with the change $\varepsilon \to \mu$. An important feature of (A1) is that it does not use the reflection factors, and the contributions from evanescent and propagating modes are not separated. Using (A1), the first-order-velocity approximation at $T_1 = T_2 = T$ yields (Eq.23) in Ref. 22)

$$F_x = \frac{\hbar V}{2\pi^2}\int_0^\infty dn(\omega) \int d^2k k_x |q|^2 [\mathrm{Im}(q_1/\varepsilon_1)\mathrm{Im}(q_2/\varepsilon_2)|Q_\varepsilon|^{-2} + \mathrm{Im}(q_1/\mu_1)\mathrm{Im}(q_2/\mu_2)|Q_u|^{-2}] \quad \text{(A2)}$$

In the case $T_1 = T_2 = 0$, from (A1) we obtain the quantum friction force [22]

$$F_x = \frac{\hbar}{4\pi^3}\int_{-\infty}^{+\infty} dk_y \int_0^\infty d\omega\, dk_x k_x \int_0^{k_x V} \exp(-2kl)\mathrm{Im}\Delta_{1\varepsilon}\mathrm{Im}\widetilde{\Delta_{2\varepsilon}}|D_\varepsilon|^{-2} + (\varepsilon \to \mu). \quad \text{(A3)}$$

Here $\Delta_{ie} = (\varepsilon_i q_i - q_i)/(\varepsilon_i q_i + q_i)$, $i = 1, 2$, $D_\varepsilon = 1 - \Delta_{1\varepsilon}\widetilde{\Delta_{2\varepsilon}}\exp(-2kl)$, and the same expressions are used for magnetic contribution $(\varepsilon \to \mu)$. Note that in this paper we consider the case of nonmagnetic materials with $\mu_{1,2} = 1$.

References

[1] M. Aspelmeyer, T.J. Kippenberg, M. Marquardt, Cavity optomechanics, Rev. Mod. Phys 86 (2014) 1391–1456.
[2] K.A. Milton, J.S. Høye, I. Brevik, The reality of Casimir friction, Symmetry 8 (2016) 29–41.
[3] G.V. Dedkov, A.A. Kyasov, Fluctuation-electromagnetic interaction under dynamic and thermal nonequilibrium conditions, Phys.-Usp 187 (2017) 559–585.
[4] A.I. Volokitin, B.N.J. Persson, Electromagnetic fluctuations at the nanoscale, Theory and applications, Springer-Verlag, Berlin, Heidelberg, 2017.
[5] G.L. Klimchitskaya, V.M. Mostepanenko, Recent measurements of the Casimir force: Comparison between experiment and theory, Proc. Peter the Great St. Petersburg Polytech. Univ. No. 1 (2015) 41, Mod. Phys. Lett A35 (2020) 2040071-6.
[6] R. Esquivel, V.B. Svetovoy, Correction to the Casimir force due to the anomalous skin effect, Phys. Rev. A69 (2004) 0621021-29.
[7] V. Despoja, M. Sunjic, L. Marusic, Microscopic theory of the noncontact van der Waals interaction: Application to layered systems, Phys. Rev B75 (2007) 045422.
[8] V. Despoja, P.M. Echenique, M. Sunjic, Nonlocal microscopic theory of quantum friction between parallel metallic slabs, Phys. Rev B83 (2011) 2054241-10.
[9] D. Reiche, D.A.R. Dalvit, K. Busch, F. Intravaia, Spatial dispersion in atom-surface quantum friction, Phys. Rev. B95 (2017) 155448.
[10] R.H. Ritchie, A.L. Marusak, The surface plasmon dispersion for an electron gas, Surf. Sci 4 (1966) 234–240.
[11] R. Nunez, P.M. Echenique, R.H. Ritchie, The energy loss of energetic ions moving near a solid surface, J. Phys. C13 (1980) 4229–4246.
[12] F. Garcia-Moliner, F. Flores, Introduction to the Theory of Solid Surfaces, Cambridge University Press, New York, 1979.
[13] F.J. Garcia de Abajo, P.M. Echenique, Wake potential in the vicinity of a surface, Phys. Rev B46 (1992) 2663–2675.
[14] G.V. Dedkov, A.A. Kyasov, Conservative–dissipative forces and heating mediated by fluctuation electromagnetic field: Two plates in relative nonrelativistic motion, Surf. Sci 604 (2010) 561–566.
[15] G.V. Dedkov, A.A. Kyasov, Electromagnetic and fluctuation-electromagnetic forces of interaction of moving particles and nanoprobes with surfaces: A nonrelativistic consideration, Phys. Solid State 44 (2002) 1729–1751.
[16] F. Intravaia, R.O. Behunin, C. Henkel, K. Busch, D.A.R. Dalvit, Failure of local thermal equilibrium in quantum friction, Phys Rev. Lett 117 (2016) 1004021-5.
[17] T.L. Ferrell, P.M. Echenique, R.H. Ritchie, Friction parameter on an ion near a metal surface, Solid. St. Commun. 32 (1979) 419–422.
[18] E.M. Lifshitz, The theory of molecular attractive forces between solids, Sov. Phys. JETP 2 (1956) 73–83.
[19] N.D. Mermin, Lindhard dielectric function in the relaxation-time approximation, Phys. Rev B1 (1970) 2362–2363.
[20] J.B. Pendry, Shearing the vacuum – quantum friction, J. Phys. Condens. Matter 9 (1997) 10301–10320.
[21] V.G. Polevoy, Tangential molecular forces between moving bodies by a fluctuating electromagnetic field, Sov. Phys. JETP 71 (1990) 1119–1124.
[22] G.V. Dedkov, A.A. Kyasov, Friction and radiative heat exchange in a system of two parallel plates moving sideways: Levin-Polevoy-Rytov theory revisited, Chin. J. Phys 56 (2018) 3002 1-11.
[23] A.I. Volokitin, Resonant photon emission during relative sliding of two dielectric plates Mod, Phys. Lett A35 (3) (2020) 20400111-8.